2019

Ledinegg Instability-Induced Temperature Excursion between Thermally Isolated, Heated Parallel Microchannels

T. A. Kingston
Purdue University

J. A. Weibel
Purdue University, jaweibel@purdue.edu

S V. Garimella
Purdue University, sureshg@purdue.edu

Kingston, T. A.; Weibel, J. A.; and Garimella, S V., "Ledinegg Instability-Induced Temperature Excursion between Thermally Isolated, Heated Parallel Microchannels" (2019). *CTRC Research Publications.* Paper 335.
http://dx.doi.org/governhttps:// doi.org/10.1016/j.ijheatmasstransfer.2018.12.017

Ledinegg Instability-Induced Temperature Excursion between Thermally Isolated, Heated Parallel Microchannels

Todd A. Kingston, Justin A. Weibel, and Suresh V. Garimella*
Cooling Technologies Research Center
School of Mechanical Engineering, Purdue University, West Lafayette, Indiana 47907 USA

Abstract

Two-phase flow through heated parallel channels is commonly encountered in thermal systems used for power generation, air conditioning, and electronics cooling. Flow boiling is susceptible to instabilities that can lead to maldistribution between the channels and thereby heat transfer performance reductions. In this study, the Ledinegg instability that occurs during flow boiling in two thermally isolated parallel microchannels is studied experimentally. A dielectric liquid (HFE-7100) is delivered to the parallel channels using a constant pressure source. Both channels are uniformly subjected to the same power, which is in increased in steps. Flow visualization is conducted simultaneously with pressure drop, mass flux, and wall temperature measurements to characterize the thermal-fluidic effects of the Ledinegg instability. When the flow in both channels is in the single-phase regime, they have equal wall temperatures due to evenly distributed mass flux delivered to each channel. Boiling incipience in one of the channels triggers the Ledinegg instability which induces a temperature difference between the two channels due to flow maldistribution. The temperature difference between the two channels

* Corresponding author
E-mail addresses: kingston@purdue.edu (T.A. Kingston), jaweibel@purdue.edu (J.A. Weibel), sureshg@purdue.edu (S.V. Garimella)

grows with increasing power until boiling incipience occurs in the second channel. The wall temperatures of both channels then reduce significantly as the flow becomes more evenly distributed. The experimentally observed temperature excursion between the channels is reported here for the first time and provides an improved understanding of the thermal performance implications of the Ledinegg instability in thermally isolated parallel channels.

Graphical Abstract

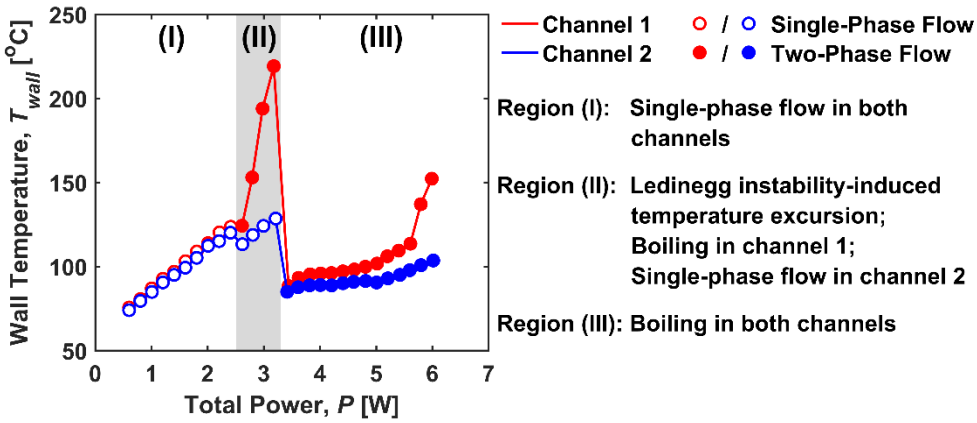

Keywords: Flow boiling, Ledinegg instability, parallel microchannels, temperature excursion, two-phase flow

Highlights

- Flow boiling in two thermally isolated parallel microchannels is studied experimentally.
- Boiling incipience in one channel triggers the Ledinegg instability.
- The Ledinegg instability induces a temperature excursion due to flow maldistribution.
- When the second channel also experiences boiling incipience, the Ledinegg instability is suppressed.

Nomenclature

c_p	specific heat
D	microchannel inside diameter
G	mass flux
h_{fg}	heat of vaporization
k	thermal conductivity
Δp	pressure drop across the microchannel
p_{in}	inlet pressure
p_{out}	outlet pressure
p_{sat}	saturation pressure of the fluid
P_{in}	heating power into the microchannel
P_{loss}	power loss to ambient
P	total power
L	microchannel length
L_{heated}	microchannel heated length
T	temperature
T_{in}	inlet fluid temperature
T_{out}	outlet fluid temperature
T_{sat}	fluid saturation temperature
T_{ref}	reference temperature
T_{wall}	microchannel outside wall temperature
V	voltage
I	electric current
Q	volumetric flow rate
q_{in}	heat flux into the fluid in the microchannel
z	axial position of the wall temperature measurement along the heated length of the microchannel

Greek Letters

ρ	density
μ	dynamic viscosity
σ	surface tension

1 Introduction

Two-phase heat sinks and evaporators used for electronics cooling and air conditioning feature many parallel channels to distribute coolant over large surface areas. Instabilities can occur during flow boiling that lead to reduced performance and, in the case of two-phase heat sinks for thermal management applications, a lower critical heat flux limit than expected from theoretical dryout [1]. Flow boiling instabilities are classified as either dynamic or static instabilities [2-5]. Flow is subjected to a dynamic instability when there is sufficient interaction between the inertia of the flow and the compressibility of the system, leading to delayed feedback. Flow is subjected to a static instability if, when disturbed, it tends asymptotically toward new operating conditions that differ from the initial conditions.

One type of static instability that has received attention over several decades is the flow excursion or Ledinegg instability [6]. This instability is characterized by a sudden reduction in flow rate and arises in flow boiling systems because of the non-monotonic nature of the channel demand curve (*i.e.*, channel pressure drop as a function of flow rate). For a single channel, the Ledinegg instability occurs when the slope of the channel demand curve becomes smaller than the slope of the supply pressure drop versus flow rate curve [2, 7]. In parallel channel systems, the Ledinegg instability results in undesirable flow maldistribution between the individual channels. Inlet restrictors have been used to mitigate the effects of flow instabilities in heated parallel channels by reducing the negative slope region of the channel demand curve [8-12]. However, doing so increases the flow resistance of the channels and the pumping power needed to sustain the flow. Akagawa *et al.* [7] experimentally investigated the Ledinegg instability in single and multiple channels. They experimentally obtained channel demand curves for individual channels undergoing flow boiling and then measured the flow rate distribution in

parallel channel configurations (up to three parallel channels). It was shown that the flow rate distribution could be estimated from the individual channel demand curves. A stability criterion was developed for systems having any number of parallel channels by linearizing the governing momentum and continuity equations and performing a Laplace transformation; this stability criterion was used to explain their experimental observations. Van Oevelen *et al.* [13] modified the approach developed in Ref. [7] to enable prediction of the flow distribution in a large number of identical parallel channels. Systems with up to 200 parallel channels were studied and it was shown that the system stability for a constant total flow rate supply curve converges asymptotically to the stability behavior for a constant pressure drop as the number of channels increases. This methodology was also used to perform a parametric study of the effects of inlet temperature, heat flux, and flow rate on the flow distribution.

While the hydrodynamic implications are well-reported [6, 7, 10, 13-19], less is known about the implications of flow maldistribution caused by the Ledinegg instability on thermal performance. Several previous studies have focused on the effect of thermal coupling between parallel channels on the mitigation of flow maldistribution resulting from the Ledinegg instability. Flynn *et al.* [20, 21] experimentally investigated two parallel microchannels that were either thermally isolated or coupled. Channels were etched into silicon and separated by either an air gap to thermally isolate the channels, or silicon to thermally couple the channels. The heat flux into each channel was independently varied for each configuration. In the thermally isolated configuration, uniform heating of the channels resulted in either single-phase flow or two-phase flow through both channels, depending on the level of heat input, and a minimal channel-to-channel temperature difference. Under severe non-uniform heating, boiling was induced in the channel with higher heating while flow through the other channel remained in

the single-phase regime, resulting in a channel-to-channel temperature difference. In the thermally coupled configuration, fluid flow through both the channels was either in the single-phase regime or underwent boiling, even at high levels of non-uniform heating. The temperature difference between the channels was relatively small due to redistribution of heat through the conductive substrate. The effect of thermal coupling between parallel channels on the flow distribution was theoretically investigated by Van Oevelen *et al.* [22] by additionally accounting for heat conduction in their previous model [13]. By quantifying the flow maldistribution in parallel-channel systems having varying strengths of inter-channel thermal coupling, it was shown that increasing thermal coupling damped the severity of the flow maldistribution. In addition, a heat flux threshold was identified below which flow maldistribution is entirely suppressed; this heat flux threshold increases as the thermal coupling increases and eventually plateaus to a constant value at very strong thermal coupling.

Notwithstanding the advantages offered by thermal coupling for reducing the flow maldistribution and channel-to-channel temperature difference, many applications utilizing flow boiling feature thermally isolated flow paths. For example, thermally isolated parallel channels are used in the renewable energy industry for direct steam generation using solar heating [23]. Additionally, multiple liquid cold plates are often arranged in a parallel configuration in the electronics cooling industry for heat rejection [24]. If two-phase operation is adopted, flow maldistribution between these thermally isolated heat sinks may be exacerbated due to the Ledinegg instability. Thus, an improved understanding of the thermal implications of the Ledinegg instability in thermally isolated parallel channels is needed.

In this study, the hydrodynamic and heat transfer characteristics of two thermally isolated parallel microchannels are studied experimentally. An experimental test facility is used to

simultaneously obtain flow visualizations and pressure drop, mass flux, and wall temperature measurements. These measurements are used to study the Ledinegg instability and experimentally demonstrate a growing temperature difference between two parallel channels with increasing power – a temperature excursion – induced by this instability.

2 Experimental Methods

2.1 Test Facility

The custom-built experimental facility, schematically illustrated in Figure 1, is adapted from our previous studies of flow boiling instabilities in a single microchannel [25, 26], and uses a pressurized reservoir to deliver degassed, dielectric HFE-7100 liquid (Novec Engineered Fluid, 3M) to two parallel microchannels. The pressure difference between the reservoir and the ambient is used to generate an open-loop flow. The rigid stainless steel reservoir is pressurized by boiling fluid using a submerged cartridge heater (G6A-15568, Watlow). Electrical power is supplied to the cartridge heater using an adjustable direct current power supply (XG 850W 150-5.6, Sorensen). A constant reservoir pressure is set and maintained by adjusting the amount of power delivered to the cartridge heater.

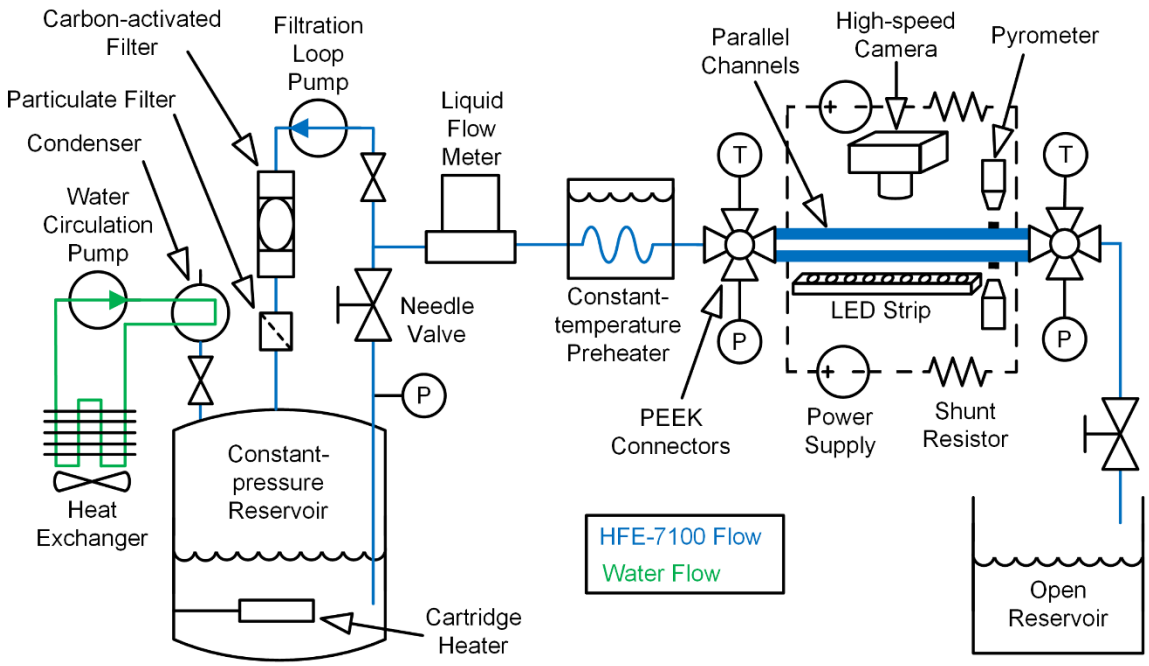

Figure 1. Schematic diagram of the experimental facility used to study the Ledinegg instability in two thermally isolated parallel microchannels.

Liquid is extracted from the reservoir through an internal dip tube. The liquid flow rate and the saturation pressure at the outlet of the microchannels are set using a pair of needle valves (FVL-404-SS and FVL-405-SS, Omega Engineering), one upstream and one downstream of the channels, respectively. The liquid volumetric flow rate and temperature are measured using a liquid flow meter (LC-10CCM-D-EPDM, Alicat; accuracy of ±1% full scale). The fluid is preheated to the desired inlet temperature immediately upstream of the microchannels using a constant-temperature circulating bath (NESLAB EX 17, Thermo Electron Corp.). The temperature of the fluid entering and exiting the microchannels is measured immediately upstream and downstream of the channels, respectively, using thermocouples (TMTSS-020E-6, Omega Engineering; ±0.5 °C). The pressures at the inlet and outlet of the microchannels are measured using separate pressure transducers (PX309-030G5V and PX309-015G5V,

respectively, Omega Engineering; ±1%), and yield the pressure drop across the microchannels. The thermocouples and pressure transducers, in addition to the fluid inlet and outlet connections, are mounted to polyetheretherketone (PEEK) connectors (ZX2LPK, Valco Instruments) which serve as inlet and outlet plenums, as shown in Figure 1; two microchannels are horizontally mounted side-by-side in parallel between these connectors.

The two identical parallel channels are circular cross-section microchannels made of borosilicate glass (CV5070, VitroCom) with an inside diameter of D = 500 μm and a wall thickness of 100 μm. The outside surface of the channels is custom-coated with an approximately 100 nm-thick layer of indium tin oxide (ITO) using atomic layer deposition (Veeco - CNT). The ITO layer is optically transparent and electrically conductive, enabling visualization of the two-phase flow while subjected to Joule heating. Power is supplied to each channel's ITO coating separately using two adjustable direct current power supplies (XG 850W 300V-2.8A, Sorensen). The ITO layers are electrically isolated from the flow loop using non-conductive polytetrafluoroethylene (PTFE) ferrules and PEEK nuts for attachment of the channels to the PEEK connectors. Any vapor leaving the channels condenses before discharging as liquid to an open reservoir at ambient pressure.

As described in Ref. [25], pressure, mass flux, and fluid temperature measurements are obtained using a data acquisition (DAQ) unit (USB-6259, National Instruments). The power to each channel is measured using a separate, high-voltage DAQ (34970A, Agilent). The total power (which includes power loss to the ambient) applied to each channel is quantified by measuring the voltage drop across and current through each of the ITO-coated channels; current measurements are obtained using two identical shunt resistors (6142-1-1000, Empro Shunts).

The entire experimental facility is mounted on a damped optical table (VIS3672-PG2-325A, Newport Corp.) to ensure that external vibrations are not transmitted to the components.

The outside wall temperature of each microchannel is measured at a single fixed location using two separate pyrometers (CTfast LT25F, Optris) coupled to focusing lenses (ACCTCF, Optris). The pyrometers feature a small spot size of 500 μm to ensure accurate, nonintrusive temperature measurement on the outside surface of the channels without obscuring visualization of the flow. Each pyrometer is focused on a black dot painted on the outside surface of a channel. The axial position of the wall temperature measurement along the heated length of the microchannel is $(z / L_{heated}) = 0.91$; the heated length of the microchannel is $L_{heated} = 42$ mm.

The entire heated region of the microchannels is visualized from the top using a high-speed camera (VEO710L, Phantom) coupled to a macro lens (AF Micro-Nikkor, Nikon) using an image resolution of 1280 × 120. The bottom side of the channels is uniformly backlit using a high-intensity light-emitting diode (LED) strip with an integrated light diffuser (BL168, Advanced Illumination).

2.2 Test Procedure

As described in Ref. [25], immediately prior to testing, the HFE-7100 fluid was degassed by vigorously boiling the liquid in the reservoir using the submerged cartridge heater. Non-condensable gases are expelled, while the HFE-7100 vapor is condensed back into the reservoir (Figure 1). While degassing, the HFE-7100 was also circulated through an auxiliary pumped filtration loop containing a 2 μm particulate filter (SS-4TF-2, Swagelok) and an activated-carbon filter (12011 Pall Corporation) to remove any contaminants. After degassing and filtering, the pumps in these auxiliary loops were turned off.

Experiments were initiated by boiling the liquid in the reservoir until it reached a constant reservoir pressure of 190 kPa. Liquid flow was then initiated through the parallel microchannels at an average mass flux of 400 kg/m^{2}s while maintaining a saturation pressure of 114 kPa at the outlet of the channels by adjusting the needle valves; this corresponds to an outlet saturation temperature of $T_{sat,out}$ = 65 °C. The test facility features a constant pressure drop across the system, not a constant mass flux, and thus the average mass flux through the microchannels can vary from the initial setting once boiling occurs and causes a change in the flow resistance. The constant-temperature bath setpoint was adjusted to heat the liquid to an inlet temperature of T_{in} = 60 °C, resulting in an inlet liquid subcooling of 5 °C, based on the outlet saturation temperature. After establishing the desired flow conditions, power was applied to the ITO-coatings of the channels in increments, allowing for steady-state conditions to be achieved at each set point. Optical images and sensor data were then acquired at steady state for 12 s.

2.3 Data Reduction

The voltages output from the pyrometers are converted to a temperature via a calibration to a target surface featuring the same black paint as used on the microchannels. The calibration temperature was varied from 20 °C to 250 °C in 10 °C increments. A linear fit of this temperature versus voltage output is used for each pyrometer to convert the measured signal during testing to a channel wall temperature. The linear fits for the pyrometers are: $T_1 = 55.69\ V_1 - 0.35$ and $T_2 = 56.98\ V_2 - 2.36$ where T_1 and T_2 are the temperatures and V_1 and V_2 are the corresponding measured pyrometer output voltages. The coefficients of determination for both linear fits were $R^2 = 1.00$.

A portion of the total power supplied to the ITO coating on each microchannel is lost to the ambient (and not transferred to the fluid through the channel wall). This power loss was

calibrated as a function of the channel wall temperatures. The wall temperatures of both channels are measured using the pyrometers during calibration; it was observed that the power loss of an individual channel is a function of only the temperature of that channel, due to thermal isolation from the other channel. A temperature-dependent power loss equation was therefore developed for each individual channel and used to quantify the power loss during testing. The heating power being dissipated by the fluid flow inside each channel is calculated by subtracting the power loss from the total electric power supplied using $P_{in} = P - P_{loss}$; the total power supplied is calculated using $P = VI$ where V is the voltage applied to the ITO coating on each channel and I is the current through the ITO coating on each channel.

The heat flux into the fluid is calculated using $q_{in} = P_{in} / (\pi D L_{heated})$. The heat transfer coefficient is calculated using $h = q_{in} / (T_{wall} - T_{ref})$, where the reference temperature (T_{ref}) is evaluated at the location of the wall temperature measurement [$(z / L_{heated}) = 0.91$]. For single-phase flow, the reference temperature is defined as the liquid temperature at this location assuming a linear increase in liquid temperature from the inlet to the outlet of the microchannel: $T_{ref} = T_{in} + (z / L_{heated})(T_{out} - T_{in})$. For two-phase flow, the reference temperature is defined as the local saturation temperature of the two-phase mixture at the location of the wall temperature measurement, $T_{ref} = T_{sat}$. A local saturation pressure is calculated assuming a linear decrease in the pressure from the inlet to the outlet of the microchannel: $p_{sat} = p_{in} - (z / L_{heated})(p_{in} - p_{out})$. The average mass flux through the two channels is calculated as $G = Q\rho / (2\pi D^2/4)$ where Q is the measured total volumetric flow rate and ρ is the calculated liquid density corresponding to the measured liquid temperature at the flow meter. Note that the mass flux through each individual channel is not measured. The pressure drop across the channels is equal and is calculated as the difference between the inlet and outlet pressures, $\Delta p = p_{in} - p_{out}$.

3 Results and Discussion

Figure 2 shows the (a) wall temperature, (b) heat flux into the fluid, and (c) heat transfer coefficient of each microchannel as a function of total power. At low power levels (P = 0 - 2.4 W), single-phase flow is observed in both channels (marked as region I in Figure 2). Under single-phase flow conditions, the wall temperatures (Figure 2a) and heat fluxes (Figure 2b) of the two channels are equal (within measurement uncertainty) and increase linearly with increasing power. An equal wall temperature at the same power indicates that both channels are receiving the same mass fluxes and thus the flow is evenly distributed by the inlet plenum. The heat transfer coefficients for both channels are correspondingly similar at each power level and remain relatively constant with increasing power throughout the single-phase regime (Figure 2c).

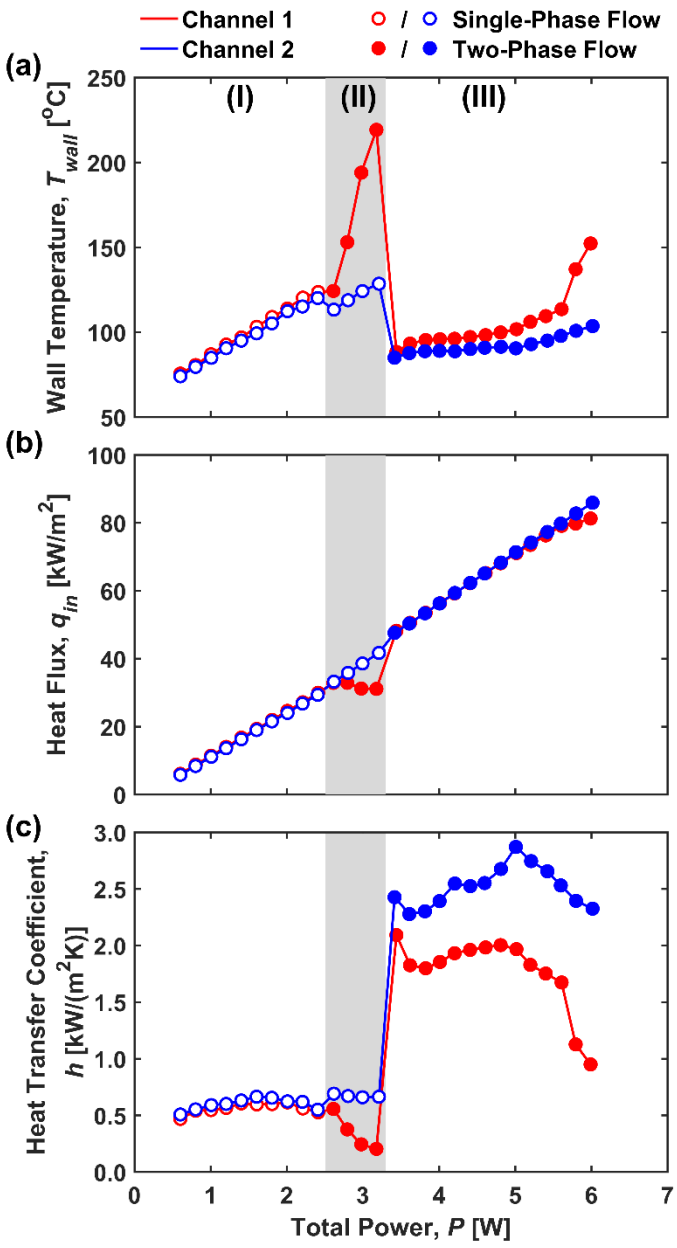

Figure 2. (a) Wall temperature, (b) heat flux into the fluid, and (c) heat transfer coefficient of each microchannel as a function of total power. The flow regime in each channel is denoted by the symbol type: Open symbols (○) for single-phase flow and closed symbols (●) for two-phase flow. The labeled regions indicate operating conditions where: (I) flow through both channels is single-phase, (II) boiling is occurring in channel 1 only, and (III) boiling is occurring in both channels.

At a power of P = 2.6 W, boiling is observed in channel 1 while channel 2 remains in the single-phase regime. After boiling incipience in channel 1, its wall temperature increases steeply with increasing power, from $T_{wall,1}$ = 124 °C at P = 2.6 W to $T_{wall,1}$ = 219 °C at P = 3.2 W (region II). In contrast, boiling incipience in channel 1 causes an initial reduction in the wall temperature of channel 2 (from $T_{wall,2}$ = 120 °C at P = 2.4 W to $T_{wall,2}$ = 113 °C at P = 2.6 W), followed by a linear increase with power (to $T_{wall,2}$ = 129 °C at P = 3.2 W); this behavior reflects an initial increase in mass flux going to channel 2 followed by single-phase operation. The range of power that causes boiling in channel 1 and single-phase flow in channel 2 is indicated as region II (gray box) in Figure 2. Once boiling in channel 1 occurs (at P = 2.6 W), the Ledinegg instability is triggered and causes flow maldistribution between the two channels (*i.e.*, a larger mass flux through channel 2 than channel 1) and a hydrodynamic excursion with increasing power, which induces a temperature excursion. While it has been shown in the literature that the Ledinegg instability can cause a temperature difference between two thermally isolated channels [21], to the authors' knowledge, the growing difference in the wall temperature of the channels with increasing power (*i.e.*, temperature excursion between the channels) has not been previously observed in experiments.

The heat flux into channel 1 decreases slightly with increasing power throughout region II (Figure 2b) because the convective thermal resistance on the inside surface of the channel increases due to the worsening flow maldistribution. Meanwhile, the heat flux into channel 2 increases linearly with increasing power throughout region II. The increase in thermal resistance for channel 1 throughout region II is reflected by the decrease in the heat transfer coefficient with increasing power (Figure 2c). A slight increase in the heat transfer coefficient for channel 2 is observed in region II relative to region I due to the increased mass flux, which causes an increase

in the length of the channel experiencing thermally developing laminar flow. It is important to note that the thermal isolation between the two channels, which restricts heat exchange from channel 1 to channel 2, prevents the equalization of heat flux in the two channels.

At P = 3.4 W, the wall temperature of channel 2 becomes large enough to cause boiling incipience in channel 2 and a significant reduction is observed in the wall temperature of both channels to T_{wall} = 85 °C. The flow resistances of the two channels become approximately equal again once both experience boiling, which reduces the flow maldistribution between the two channels and suppresses the temperature excursion induced by the Ledinegg instability. When both channels experience boiling (region III), the heat fluxes to each channel are again equal at each power level (Figure 2b). The steep reduction in wall temperatures upon boiling incipience in channel 2 is reflected in the large increase seen in the heat transfer coefficients (Figure 2c). The wall temperatures and heat transfer coefficients are relatively constant throughout region III until P = 5.8 W when the wall temperature of channel 1 begins to increase with power, likely due to intermittent dryout.

The flow in both microchannels was visualized at each power level. Figure 3 shows a selected image obtained by the high-speed camera and an accompanying schematic representation of the flow regime in the two parallel channels. The flow direction is from left to right. The entire heated length of the channels is shown in the images; the electrical connections to the ITO coating are just outside the viewing region. The mass flux to each channel in each of the three regions is qualitatively represented by the length of the arrows near the channel inlets. The flow visualizations captured at each power level, and those selected in Figure 3, enable the two-phase morphology to be identified and support the trends shown in Figure 2. That is, three different regions exist depending on the operating conditions, where (I) both channels are in the

single-phase flow regime, (II) boiling is observed in channel 1 and single-phase flow is observed in channel 2, or (III) both channels are boiling.

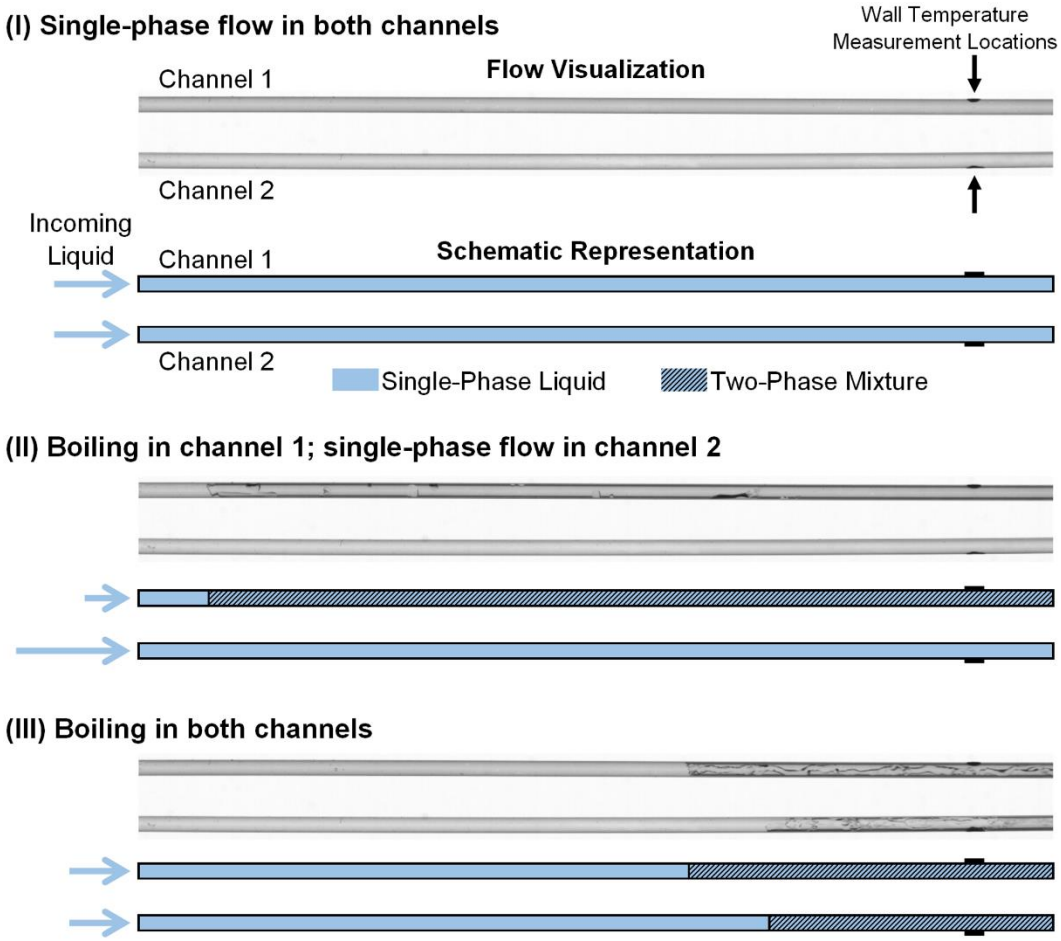

Figure 3. Flow visualization images and accompanying schematic representations of the flow regime observed in each channel for (I) single-phase flow in both channels, (II) boiling in channel 1 and single-phase flow is in channel 2, and (III) boiling in both channels. The flow direction is from left to right.

While the two parallel microchannels are thermally isolated, they are hydrodynamically coupled through the same inlet and outlet plenums, resulting in a common pressure drop. However, because of the non-monotonic nature of the channel demand curve, the mass flux through the channels can differ significantly, even with the same pressure drop. While the mass

flux through each individual channel cannot be measured, an average mass flux is measured using the upstream flow meter, thus providing an indication of the overall flow resistance of the two parallel channels. Figure 4 shows the (a) pressure drop and (b) average mass flux of the two channels as a function of total power. At low power levels (P = 0 - 2.4 W) when both channels are in the single-phase flow regime (region I), the pressure drop remains fairly constant at 2 kPa and the average mass flux through both channels is 400 kg/m^{2}s. Once boiling occurs in channel 1 at P = 2.6 W, the flow resistance increases and the pressure drop increases to approximately 3.5 kPa within region II. The additional flow resistance caused by boiling in channel 1 does not significantly increase the pressure drop because fluid is rerouted to channel 2, which is still in the single-phase regime. Thus, the average mass flux through the channels only reduces slightly. A minimal increase in pressure drop was also noted by Flynn *et al.* [21] when boiling occurred in only one of the two parallel channels. At P = 3.4 W, when boiling starts occurring in both channels, the pressure drop increases significantly to 11.7 kPa and the average mass flux reduces to 368 kg/m^{2}s. Throughout region III, the pressure drop increases with increasing power due to the increased flow resistance associated with vapor generation within both channels. As a result, the average mass flux also reduces with increasing power.

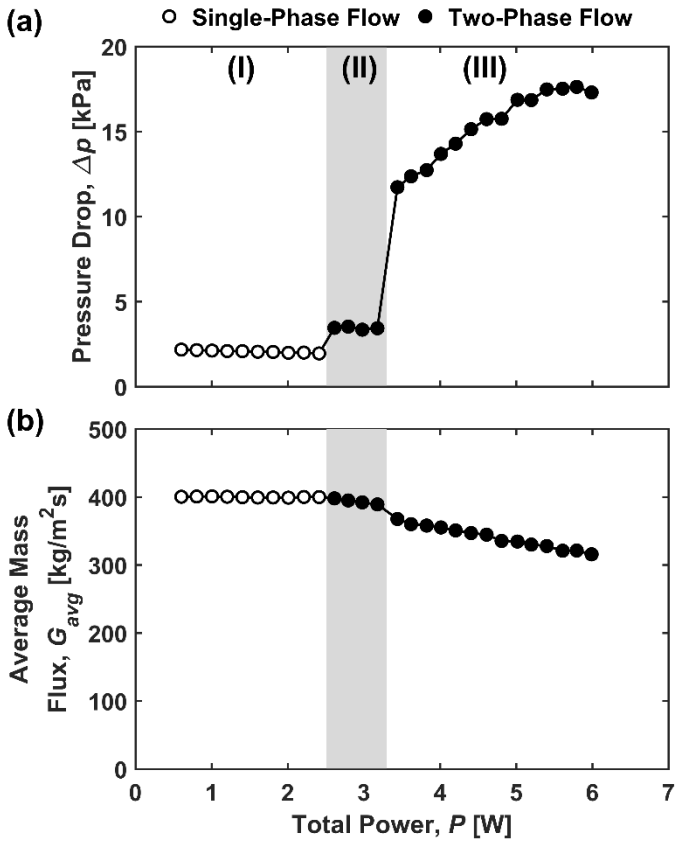

Figure 4. (a) Pressure drop across and (b) average mass flux through the two microchannels as a function of total power. Open symbols (○) denote single-phase flow in both channels and closed symbols (●) denote that at least one channel is boiling.

4 Conclusions

In this study, the Ledinegg instability and its influence on the thermal performance of a parallel microchannel system are experimentally investigated. HFE-7100 liquid is delivered to two thermally isolated parallel channels using a constant pressure source. Both channels are uniformly subjected to the same power, which is increased in steps. High-speed flow visualization is synchronized with pressure drop, mass flux, and wall temperature measurements. When the flow in both channels is in the single-phase regime, the mass flux to each channel is approximately equal. At a power level sufficient to cause boiling incipience in one of the

channels, the flow resistance in that channel increases and triggers the Ledinegg instability which causes severe flow maldistribution. With increasing power to the channels, the Ledinegg instability triggers a temperature excursion, causing the wall temperature of the flow-starved channel (experiencing boiling) to increase along with a correspondingly deteriorating heat transfer coefficient. The temperature excursion continues until boiling incipience occurs in the second channel, after which the maldistribution reduces and the wall temperature of both channels reduces significantly. This study illustrates the thermal implications of the Ledinegg instability in thermally isolated parallel channels and provides new understanding of the mechanisms leading to the observed temperature excursion.

Acknowledgments

This research is sponsored by the Naval Engineering Education Consortium (NEEC), with support of Naval Surface Warfare Center (NSWC) Crane Division in Crane, Indiana. Special thanks to Dr. Brian D. Olson (NSWC Crane Division) for technical discussions related to this work.

References

[1] A.E. Bergles, S.G. Kandlikar, On the nature of critical heat flux in microchannels, *Journal of Heat Transfer*, 127(1) (2005) 101-107.

[2] J.A. Boure, A.E. Bergles, L.S. Tong, Review of two-phase flow instability, *Nuclear Engineering and Design*, 25(2) (1973) 165-192.

[3] L.C. Ruspini, C.P. Marcel, A. Clausse, Two-phase flow instabilities: A review, *International Journal of Heat and Mass Transfer*, 71 (2014) 521-548.

[4] L. Tadrist, Review on two-phase flow instabilities in narrow spaces, *International Journal of Heat and Fluid Flow*, 28(1) (2007) 54-62.

[5] S. Kakac, B. Bon, A review of two-phase flow dynamic instabilities in tube boiling systems, *International Journal of Heat and Mass Transfer*, 51(3-4) (2008) 399-433.

[6] M. Ledinegg, Instability of flow during natural and forced circulation, *Die Warme*, 61(8) (1938) 891-898.

[7] K. Akagawa, M. Kono, T. Sakaguchi, M. Nishimura, Study on distribution of flow rates and flow stabilities in parallel long evaporators, *Bulletin of Japan Society of Mechanical Engineers*, 14(74) (1971) 837-848.

[8] Y.K. Prajapati, P. Bhandari, Flow boiling instabilities in microchannels and their promising solutions - A review, *Experimental Thermal and Fluid Science*, 88 (2017) 576-593.

[9] A. Koşar, C.J. Kuo, Y. Peles, Suppression of boiling flow oscillations in parallel microchannels by inlet restrictors, *Journal of Heat Transfer*, 128(3) (2006) 251-260.

[10] T. Zhang, T. Tong, J.-Y. Chang, Y. Peles, R. Prasher, M.K. Jensen, J.T. Wen, P. Phelan, Ledinegg instability in microchannels, *International Journal of Heat and Mass Transfer*, 52(25–26) (2009) 5661-5674.

[11] S.G. Kandlikar, W.K. Kuan, D.A. Willistein, J. Borrelli, Stabilization of flow boiling in microchannels using pressure drop elements and fabricated nucleation sites, *Journal of Heat Transfer*, 128(4) (2006) 389-396.

[12] A. Mukherjee, S.G. Kandlikar, The effect of inlet constriction on bubble growth during flow boiling in microchannels, *International Journal of Heat and Mass Transfer*, 52(21-22) (2009) 5204-5212.

[13] T. Van Oevelen, J.A. Weibel, S.V. Garimella, Predicting two-phase flow distribution and stability in systems with many parallel heated channels, *International Journal of Heat and Mass Transfer*, 107 (2017) 557-571.

[14] S. Natan, D. Barnea, Y. Taitel, Direct steam generation in parallel pipes, *International Journal of Multiphase Flow*, 29(11) (2003) 1669-1683.

[15] U. Minzer, D. Barnea, Y. Taitel, Evaporation in parallel pipes-splitting characteristics, *International Journal of Multiphase Flow*, 30(7-8) (2004) 763-777.

[16] U. Minzer, D. Barnea, Y. Taitel, Flow rate distribution in evaporating parallel pipes - modeling and experimental, *Chemical Engineering Science*, 61(22) (2006) 7249-7259.

[17] M. Baikin, Y. Taitel, D. Barnea, Flow rate distribution in parallel heated pipes, *International Journal of Heat and Mass Transfer*, 54(19-20) (2011) 4448-4457.

[18] D. Barnea, M. Simkhis, Y. Taitel, Transient data for flow of evaporating fluid in parallel mini pipes and comparison with theoretical simulations, *International Journal of Multiphase Flow*, 77 (2015) 58-64.

[19] L.C. Ruspini, C.A. Dorao, M. Fernandino, Dynamic simulation of Ledinegg instability, *Journal of Natural Gas Science and Engineering*, 2(5) (2010) 211-216.

[20] R.D. Flynn, D.W. Fogg, J.-M. Koo, C.-H. Cheng, K.E. Goodson, Boiling flow interaction between two parallel microchannels, in: Proceedings of ASME IMECE, Chicago, Illinois, USA, 2006, pp. 317-322.

[21] R. Flynn, C.-H. Cheng, K. Goodson, Decoupled thermal and fluidic effects on hotspot cooling in a boiling flow microchannel heat sink, in: Proceedings of ASME InterPACK, Vancouver, British Columbia, Canada, 2007, pp. 179-184.

[22] T. Van Oevelen, J.A. Weibel, S.V. Garimella, The effect of lateral thermal coupling between parallel microchannels on two-phase flow distribution, *International Journal of Heat and Mass Transfer*, 124 (2018) 769-781.

[23] T. Hirsch, J.F. Feldhoff, K. Hennecke, R. Pitz-Paal, Advancements in the field of direct steam generation in linear solar concentrators - A review, *Heat Transfer Engineering*, 35(3) (2014) 258-271.

[24] R.C. Chu, R.E. Simons, M.J. Ellsworth, R.R. Schmidt, V. Cozzolino, Review of cooling technologies for computer products, *IEEE Transactions on Device and Materials Reliability*, 4 (2004) 568-585.

[25] T.A. Kingston, J.A. Weibel, S.V. Garimella, High-frequency thermal-fluidic characterization of dynamic microchannel flow boiling instabilities: Part 1 - Rapid-bubble-growth instability at the onset of boiling, *International Journal of Multiphase Flow*, 106 (2018) 179-188.

[26] T.A. Kingston, J.A. Weibel, S.V. Garimella, High-frequency thermal-fluidic characterization of dynamic microchannel flow boiling instabilities: Part 2 - Impact of operating conditions on instability type and severity, *International Journal of Multiphase Flow*, 106 (2018) 189-201.